Oncogene (2017), 1–11

www.nature.com/onc

ORIGINAL ARTICLE

C-Met/miR-130b axis as novel mechanism and biomarker for castration resistance state acquisition

A Cannistraci[1,9], G Federici[1,2,9], A Addario[1], AL Di Pace[1,3], L Grassi[1,2], G Muto[4,5], D Collura[4], M Signore[1], L De Salvo[2], S Sentinelli[2], G Simone[2], M Costantini[2], S Nanni[6], A Farsetti[7], V Coppola[1], R De Maria[8,9] and D Bonci[1,2,9]

Although a significant subset of prostate tumors remain indolent during the entire life, the advanced forms are still one of the leading cause of cancer-related death. There are not reliable markers distinguishing indolent from aggressive forms. Here we highlighted a new molecular circuitry involving microRNA and coding genes promoting cancer progression and castration resistance. Our preclinical and clinical data demonstrated that c-Met activation increases miR-130b levels, inhibits androgen receptor expression, promotes cancer spreading and resistance to hormone ablation therapy. The relevance of these findings was confirmed on patients' samples and by *in silico* analysis on an independent patient cohort from Taylor's platform. Data suggest c-Met/miR-130b axis as a new prognostic marker for patients' risk assessment and as an indicator of therapy resistance. Our results propose new biomarkers for therapy decision-making in all phases of the pathology. Data may help identify high-risk patients to be treated with adjuvant therapy together with alternative cure for castration-resistant forms while facilitating the identification of possible patients candidates for anti-Met therapy. In addition, we demonstrated that it is possible to evaluate Met/miR-130b axis expression in exosomes isolated from peripheral blood of surgery candidates and advanced patients offering a new non-invasive tool for active surveillance and therapy monitoring.

Oncogene advance online publication, 13 February 2017; doi:10.1038/onc.2016.505

INTRODUCTION

Prostate cancer (PCa) is a highly frequent tumor type in men.[1,2] Many tumors are indolent, but the absence of reliable molecular bio-indicators of high-risk progression causes overtreatment of patients who are driven to radical prostatectomy. This approach, however, is not curative for the 30% of treated patients who develop advanced forms after few years. Biochemical recurrence is the first evidence of cancer progression and it is treated by hormone ablation, indicated as hormone therapy (HT).[3] Recently, new drugs, such as enzalutamide and abiraterone acetate, were approved for the treatment of castration-resistant cancer.[4,5] Although the last-generation drugs represent a considerable advance in hormonal therapy and are initially effective in blocking tumor growth, a consistent percentage of patients eventually recur for the development of lethal drug-resistant disease. The possible mechanisms to explain resistance to HT can be separated into three general categories.[6–8] The first includes DNA-based alterations in the androgen receptor (AR) gene, such as amplification or point mutations.[9–14] The second group includes ligand-independent AR activation in the absence of mutations or amplification.[15–18] The third type is associated with aberrant activation of alternative signaling pathways able to bypass AR activity, which is no longer relevant to disease progression.[19,20] The role of AR in late-stage disease progression and molecular mechanisms driving castration resistance state acquisition is still mainly debated. Recent evidence shows that AR can negatively control c-Met, a key gene associated with metastasis formation.[21,22] Compelling evidence demonstrates central role of microRNAs (miRNAs, miRs) in cancer development.[23–25] Of note, c-Met overexpression is associated with the deregulation of miRNAs in cancer.[26] We hypothesized that aberrant balance in the activity of AR/c-Met may cause a cascade of events that promotes cancer progression through miRNA profile perturbation. In this context, androgen ablation therapy, while attenuates AR aberrant activity, can de-repress c-Met transcription with consequent activation of its signaling cascade and acquisition of castration-resistant state.[22] Here we investigated the function of Met/AR axis and miRNA deregulation in PCa. We discovered a new circuitry where c-Met can control AR transduction taking advantage of miR-130b activity. Our data may provide new mechanisms of HT escaping, while highlighting novel molecular indicators for the identification of patients who will develop advanced forms and benefit of specific therapy. We propose that current androgen ablation treatment may be beneficial when combined with therapeutic strategies to inhibit the activation of the HGF/c-Met pathway in candidate patients. As the miRNA analysis can be performed in biological fluids, our data may suggest innovative non-invasive approach for follow-up monitoring.

[1]Department of Hematology, Oncology and Molecular Medicine, Istituto Superiore di Sanità, Rome, Italy; [2]Regina Elena National Cancer Institute, Rome, Italy; [3]Department of Anatomical, Histological, Forensic & Orthopaedic Sciences, Histology and Medical Embryology Section, Sapienza University of Rome, Rome, Italy; [4]Department of Urology, S. Giovanni Bosco Hospital, Turin, Italy; [5]Department of Urology, Campus Biomedico University, Rome, Italy; [6]Institute of Medical Pathology, Università Cattolica, Rome, Italy; [7]National Research Council (CNR), Institute of Cell Biology and Neurobiology, Rome, Italy and [8]Institute of General Pathology, Università Cattolica and Policlinico Gemelli, Rome, Italy. Correspondence: Professor R De Maria, Institute of General Pathology, Università Cattolica and Policlinico Gemelli, Largo Francesco Vito 1, Rome 00168, Italy or Professor D Bonci, Department of Hematology, Oncology and Molecular Medicine, Istituto Superiore Sanità, viale Regina Elena 299, Rome 00161, Italy.
E-mail: ruggero.demaria@unicatt.it or desiree.bonci@iss.it
[9]These authors contributed equally to this work.
Received 13 June 2016; revised 6 November 2016; accepted 29 November 2016

RESULTS

AR and c-Met expression in PCa cell lines

Verras *et al*. showed dual role of AR activity, suggesting that current androgen ablation therapy repressing AR activity can impair growth-promoting genes, but on the other hand, promotes de-repression of oncogenes, such as c-Met.[21,22] We further investigated the association between the two receptors and the implication in castration resistance state and metastasis development. We analyzed the expression of both c-Met/AR receptors in PCa cell lines representative of PCa different phases (Table 1). c-Met receptor was found overexpressed in basal and highly metastatic cells (Figure 1a),[27,28] whereas c-Met-negative and low-expressing LNCaP and 22Rv1 cells, respectively, expressed high level of AR (Figure 1b). Similar results were observed at the RNA level through quantitative real-time PCR (qRT-PCR; Supplementary Figures 1a and b). c-Met signaling cascade activation was documented as the expression of phosphorylated form in the highly metastatic PC-3 cell line by immunofluorescence analysis[29] (Supplementary Figure 1c), suggesting that aberrant activity of the receptor correlates with aggressive PCa forms. In line with data from literature showing increased c-Met expression in bone metastases,[30–32] c-Met messenger RNA resulted expressed in patients' metastatic tissues by *in silico* elaboration of a published gene data set reported by Taylor *et al*.[33] (Supplementary Figure 1d). Moreover, we confirmed c-Met expression in four bone metastasis tissues that resulted 3/4 medium-high and 1/4 low c-Met expressing (Figure 1c). These data support the hypothesis that c-Met could have a role in PCa progression and may be a therapeutic target in the advanced phases of disease.

C-Met overexpression in LNCaP cells and microRNA profiling

We hypothesized that c-Met/AR-deregulated axis could promote prostate tumor progression. To investigate the effect of c-Met activation, we chose AR-positive LNCaP cell line, which forms subcutaneous and orthotopic lesions when injected in immunocompromised mice, but it is unable to form metastatic foci. We transiently transfected cells with an engineered plasmid carrying a constitutive activated c-Met (TPR-MET) or its relative control (pBABE).[34,35] Receptor overexpression was confirmed by qRT-PCR (data not shown) and Western blot assay (Figure 1d), which detected high levels of the phophorylated c-Met form (p-Met). We analyzed cells after 48 h from transfection and found a significant reduction of AR at protein and messenger RNA levels when compared with control population (pBABE), providing evidences for a novel mechanism of regulation of c-Met on AR gene (Figure 1d; Supplementary Figure 1e). We speculated that c-Met activity could be mediated by miRNA gene family. We evaluated miRNA perturbation by constitutive activated c-Met in LNCaP/TPR-MET cells using TaqMan Array Cards, which guarantee accurate quantification of 754 human microRNAs (Figure 1e and Excel file). Only miRs with more than twofold changed level were considered as perturbed by c-Met expression. We compared this list with miRs able to bind the 3′-untranslated region (UTR) of AR (Table 2) as by *in silico* analysis performed with microRNA-targeting prediction software TargetScan (v5.2). When we compared the list of miRNAs able to directly bind AR with the list of miRNA upregulated by c-Met constitutive activation, we found only miR-130/301 family and miR-30b as possible candidates. Only twofold changed miRs were considered for further analysis (Supplementary Figure 1f). We excluded miR-454, which belongs to miR-130/301 family, but was not perturbed by c-Met expression (Supplementary Excel file). For the candidate miRs, we ran a bioinformatics analysis on the public gene bank data set.[33] Among listed miRs, only miR-130b resulted significantly upregulated in tumor tissues (Figure 1f; Supplementary Figure 1g). We confirmed these results with a further pivotal analysis evaluating miR-130b expression level in tissues of patients with PCa. We microdissected (only tumor cells were laser dissected) nine formalin-fixed paraffin-embedded primary tumors and three normal tissues, and evaluated miR-130b level by qRT-PCR, using normal pooled tissues as reference. We found increased levels of miR-130b in five of nine patients (Supplementary Figure 2a). We confirmed that c-Met constitutively active form expression induced miR-130b level increase in LNCaP/TPR-MET cells by qRT-PCR single assay (Supplementary Figure 2b). Non-neoplastic RWPE-1 cells were used as internal control. We next investigated whether miR-130b could directly regulate AR expression (Figure 1g). We demonstrated

Table 1. List of prostate cancer cell lines representative of tumor different phases

Cell line	*Organism*	*Tissue*	*Derivation*
RWPE-1	*Homo sapiens*	Prostate	Epithelial cells derived from the peripheral zone of a histologically normal adult human prostate
RWPE-2	*Homo sapiens*	Prostate	From RWPE-1 transformation with Ki-ras
22Rv1	*Homo sapiens*	Prostate	Prostate carcinoma, derived from a xenograft
LNCaP	*Homo sapiens*	Prostate	Metastatic site
PC-3	*Homo sapiens*	Prostate	From a bone metastasis of a grade IV prostatic adenocarcinoma

Figure 1. (**a**) Flow cytometric analysis of c-Met expression in prostate cancer cell lines. Gates were set based on isotype control staining. (**b**) Western blot analysis of AR expression level in prostate cancer cell lines. (**c**) Representative images of two bone metastasis samples of four patients stained with anti-Met antibody were reported by immunohystochemistry. Sample 1 (×10 upper panel) and (×20 lower panel) cytoplasmic staining; sample 2 (×20 upper) and (×40 lower panel) cytoplasmic and several areas of nuclear staining. Scale bars represent 30 μm. (**d**) Western blot analysis of AR and p-Met expression in control (pBABE) and MET-overexpressing LNCaP cells (TPR-MET). β-Tubulin was used as a loading control. Histogram data are shown as mean ± s.d. of three independent experiments. Unpaired T-test was used for significance. (**e**) Hierarchical clustering based on miRNA expression profiles in control (pBABE) versus Met-overexpressing LNCaP cells (TPR-MET) by MeV 4.8 software. LNCaP cells were used as reference and miRNA levels were reported as values between 0 and 1, and ⩾ 3. For additional details, see Excel file. (**f**) *In silico* analyses conducted on Taylor's data set from GEO record GSE21036. Box plots representing miR-130b expression values in normal tissues ($n = 28$) versus tumor tissues ($n = 113$ composed of 99 primary tumors and 14 metastases). (**g**) Representative scheme of miR-130b-binding site in AR 3′-UTR (nucleotides 71–77). (**h**) Luciferase assay on 293T cells transfected with renilla luciferase and with either empty pGL3 vector or a plasmid carrying the 3′-UTR of AR (pGL3 UTR–AR), in the presence of negative control scramble pre-miR or miR-130b mimic oligo. Firefly luciferase activities are normalized over renilla luciferase. Graphical data are shown as mean ± s.d. of three independent experiments. (**i**) Representative Western blot analysis of AR expression level after transfection of LNCaP cells with miR-130b mimic oligo. Nucleolin (NCL) was used as a loading control.

the direct binding of miR-130b on AR 3′-UTR in transfected 293T cells. As shown in Figure 1h, miR-130b mimic was able to reduce luciferase activity of the construct carrying the AR 3′-UTR, whereas no effects were observed in cells transduced with the empty vector. Similar results were obtained using PC-3 as recipient cells (Supplementary Figure 2c). In fact, transfection of naive PC-3 cells results in a reduction of luciferase activity, as a consequence of the endogenous levels of miR-130b, which was rescued when a synthetic anti-miR-130b was added to the cells. To verify the involvement of miR-130b in the direct regulation of AR receptor, we transiently transduced LNCaP cells with a synthetic miR-130b mimic. As shown in Figure 1i, ectopic expression of miR-130b was

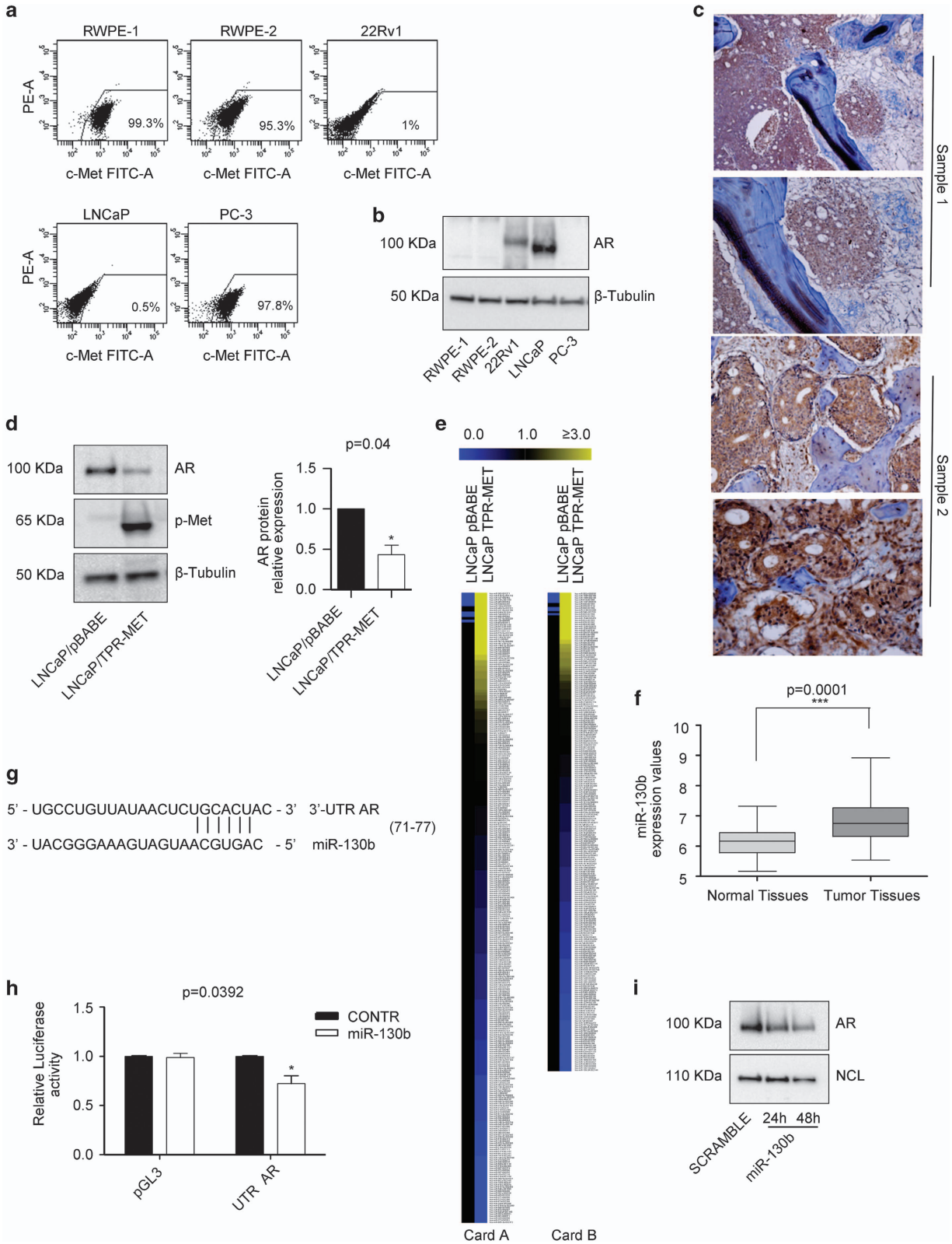

able to reduce AR protein expression, whereas the SCRAMBLE oligo did not affect the protein level. All together, these results confirmed and validated AR as a direct target of miR-130b. Thus, we focused subsequent investigation on miR-130b, which was previously reported as an oncomiR promoting epithelial-mesenchymal transition, metastasis signaling and the acquisition of a stem-like phenotype.[36–38] We speculated that c-Met could directly regulate miR-130b expression. We transfected PC-3 cells with siRNAs specific for MET gene (siRNA_MET 5# and siRNA_MET#6). Of note, in parallel to c-MET gene reduction, we found a significant decrease of miR-130b level by RT-PCR assay (Supplementary Figure 2d), whereas PC-3 cells treated with siRNA_MET#6 showed impaired growth (Supplementary Figure 2e). Two potential promoter regions of miR-130b were selected from human genome and cloned into pGL3 -Basic vector. We transiently transfected the activated form of c-MET together with two regions into 293T cells. C-Met activation enhanced the luciferase activity of the longer region demonstrating a direct control on miR-130b transcription (Supplementary Figure 2f). To verify whether the c-Met protein complex was directly involved in miR-130b regulation at

Table 2. List of miRs able to bind the 3′-untranslated region of AR (Human AR 3′-UTR (436 bp)) as by *in silico* analysis performed with microRNA-targeting prediction software TargetScan (v5.2)

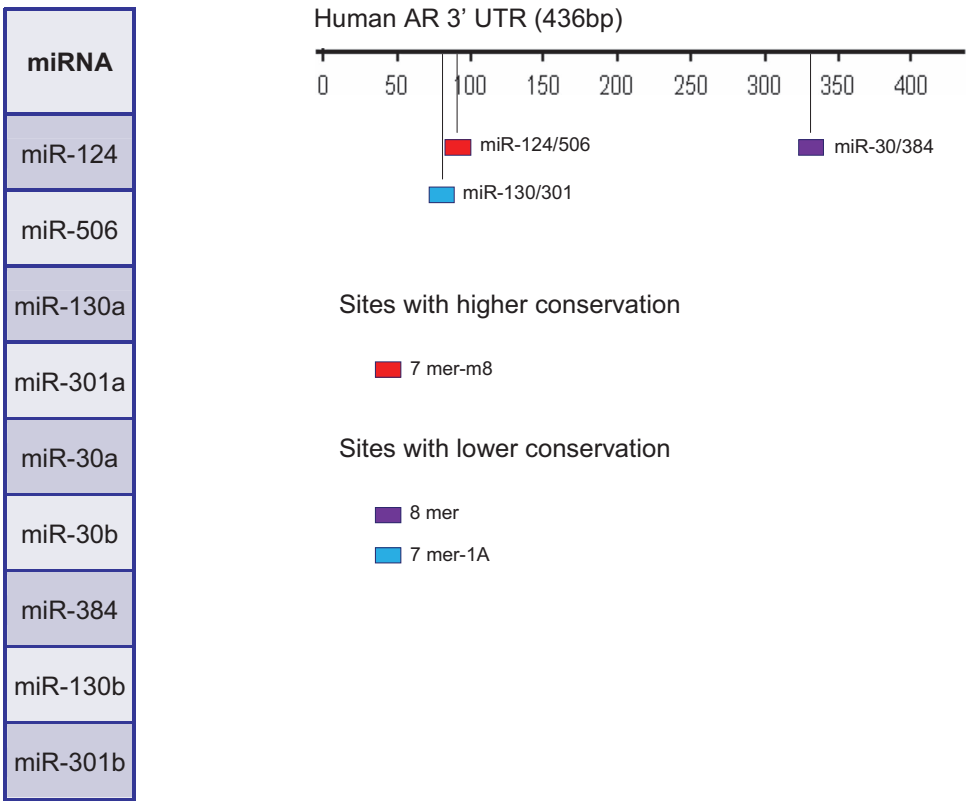

TargetScan predicts biological targets of miRNAs by searching for the presence of conserved 8mer, 7mer and 6mer sites that match the seed region of each miRNA (Lewis *et al.*, 2005).[58] Site type: 8mer: an exact match to positions 2–8 of the mature miRNA (the seed+position 8) followed by an 'A'; 7mer-m8: an exact match to positions 2–8 of the mature miRNA (the seed+position 8); 7mer-A1: an exact match to positions 2–7 of the mature miRNA (the seed) followed by an 'A'.

Figure 2. (**a**) Bioinformatic analyses conducted on data from GEO record GSE21036. Box plots representing miR-130b expression values in: normal tissues ($n=28$) versus tumor tissues ($n=99$) and metastatic tissues ($n=14$). (**b**) Patients with low/intermediate Gleason score ($n=86$) and high Gleason score ($n=12$) and (**c**) patients with intermediate T2-stage ($n=68$) and high T3/4-stage ($n=31$). Mann–Whitney *U*-test was used to determine significance in all the analyses. (**d**) miR-130b expression level in macrodissected tumor areas (tumor areas >70% of the total tissues were included) from 19 patients with at least 10 years documented follow-up, evaluated by real-time PCR. (**e**) p-Met protein levels by RPPA in exosomes of healthy donors ($n=16$) versus patients with localized tumors ($n=12$) and (**f**) miR-130b expression levels by real-time PCR in exosomes of healthy donors ($n=6$) versus patients with localized tumors ($n=12$). In **e**, *P*-value was evaluated by Wilcoxon (JMP software) two-group non-parametric test. In **f**, unpaired *T*-test was used to determine significance. The mean of healthy donors was used as reference and calculated at 1. (**g**) RPPA analysis of Met signaling cascade evaluated in exosomes isolated from 12 healthy donors (blue) and 12 patients with tumor (yellow). Heat-map shows the cluster of samples based on relative expression and was normalized as reported in Material and Methods. (**h**) p-Met protein levels by RPPA in exosomes of healthy donors ($n=5$) versus patients with primary tumors ($n=9$; tumors) and patients with castration-resistant forms ($n=9$). *P*-value was evaluated by Kruskal–Wallis/Steel–Dwass >two-group non-parametric test (JMP software).

transcriptional level, we ran a chromatin immuno precipitation (ChIP) assay in two highly Met/miR-130b-expressing cell models, the PC-3 line and the C11IM cell line established *ex vivo* and published by Nanni *et al.*[39] (Supplementary Figure 5). We hypothesized a direct involvement of p-Met or SP1 transcriptional factor, frequently involved in c-Met signal cascade activation.[40] We therefore performed the assay along a 5-kb region of the miR-130b promoter and chromatins were

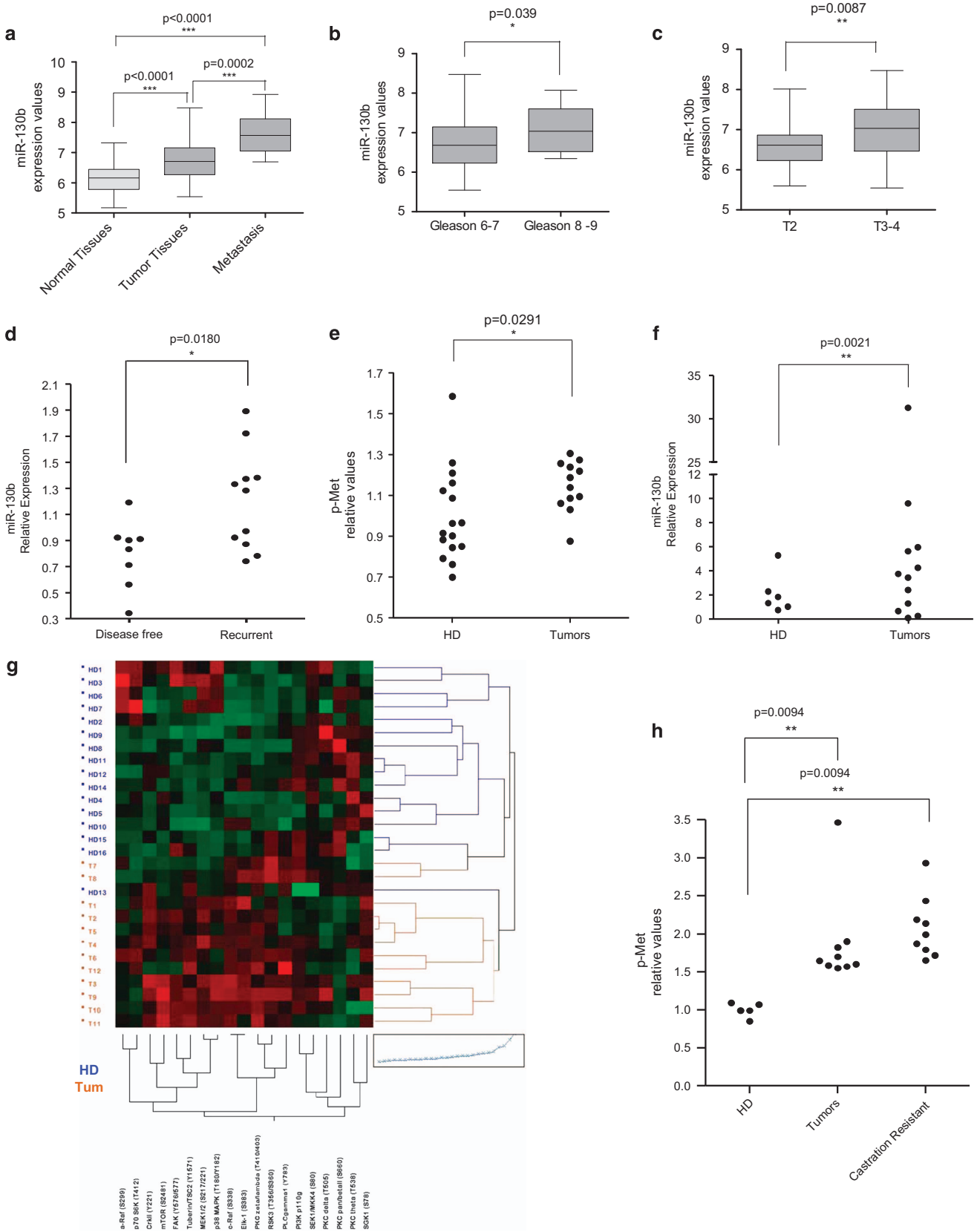

immunoprecipitated by antibodies to phosphoMET (p-Met), SP1 and anti-acetyl-histone H3 (H3Ac). We analyzed two regions, one external (green arrow, I) and one internal region (red arrow, II) to the 2 K promoter region (Supplementary Figure 3a). DNA sequences proximal to transcriptional start site (TSS) and SP1-binding sites (site II) or upstream region (outside the proximal 2 kb promoter used in luc-reporter assay, site I) were amplified. Of note, a strong recruitment of p-Met on both sites was observed in both PC-3 and C11IM cell line (Supplementary Figures 3b and c) while SP1 occupancy peaked at TSS/SP1 sites (site II versus site I). Furthermore, a strong increase (70–150-fold over control, NoAb) was observed in histone H3 acetylation density region surrounding the putative TSS, thus indicating a gene locus actively transcribed in both cell lines. Results showed a direct involvement of both p-Met and SP1 in a complex competent to transactivate miR-130b promoter. In particular, the internal region (red arrow, II) showed the strongest binding and contained the TSS indicating, in parallel with Luciferase assay, the miR-130b regulatory region. Of note, these data documented for the first time a direct involvement of p-Met as direct actor of a complex able to transactivate genome sequences in the nucleus. This is in line with immunohystochemistry images where Met staining has a cytoplasmatic and nuclear pattern (Figure 1c). To demonstrate a potential therapeutic application of our results, we evaluated the existence of a pharmacological correlation between c-Met and miR-130b. We treated PC-3 cells with SU11274 and Crizotinib, two different c-Met tyrosine kinase inhibitors, and observed a consistent reduction of endogenous level of miR-130b after treatment (Supplementary Figure 2g). These results suggested a novel molecular circuitry involving c-Met, AR and miR-130b, and proposed c-Met/miR-130b as possible candidate biomarkers for assessing response to treatment with inhibitors of c-Met kinase activity.

MiR-130b expression in PCa patients

By performing a bioinformatic analysis on Taylor's gene platform, we discovered a significant high expression of miR-130b in metastatic tissues when compared with primary tumors and normal samples (Figure 2a). Moreover, there was a significant correlation between prostate-specific antigen levels and expression of miR-130b (Supplementary Figure 2h) in primary tumors. These data suggested a direct correlation between increased miR-130b level and tumor progression. Furthermore, miR-130b high level significantly correlated with clinical risk parameters, such as high Gleason score and pT (Figures 2b and c). We selected 19 patients with at least 10 years documented follow-up from our tissue bank. Following the same technical approach used in Taylor's paper, we macrodissected tumor areas (tumor areas $>70\%$ of the total tissues were included) and analyzed miR-130b expression. We found that patients experiencing tumor recurrence displayed higher levels of miR-130b in primary tumors as compared with tumor-free patients after 10 years (Figure 2d). As it is well documented that formalin-fixed paraffin-embedded tissues are not reliable samples for evaluation of protein phosphorylation,[41,42] we could not evaluate p-Met activation in the same patients. As molecular analysis of exosomes may provide prognostic and predictive clinical indications,[43–45] we analyzed exosomes released into the blood stream to investigate p-Met expression in patients sera collected before prostatectomy. We isolated exosomes by multiple rounds of ultracentrifugation and evaluated p-Met levels by a sensible technique, the reverse-phase protein array (RPPA).[46] The analysis of exosomes from PCa patients and healthy donors showed that p-Met was present at higher level in circulating exosomes from patients (Figure 2e). We also evaluated the expression of miR-130b in exosomal samples. Similarly to the observation in tumor tissues, miR-130b was upregulated in exosomes from PCa patients as compared with healthy donor samples (Figure 2f). Thus, our data demonstrated a general and significant increase of p-Met and miR-130b in PCa patients, and proposed that it might be possible to monitor their increase with a non-invasive approach using nanovesicles isolated from peripheral blood of patients. We then extended the analysis by RPPA assay on proteins associated with Met signaling cascade on 16 healthy donors (HDs) and 12 tumors (T1-12). We found a significant activation of the Met signaling cascade in patients with tumors, suggesting that it is theoretically possible to follow the signaling activation through the monitoring of several key proteins (Figure 2g; Supplementary Figures 4a–c). We extended the analysis to an additional set of samples, including primary tumor and castration-resistant patients (Figure 2h). We isolated exosomes from sera and analyzed p-Met expression by RPPA assay. We demonstrated that it is possible to analyze the protein pattern in exosomes isolated from patients with recurrence, where tumor metastatic material is not disposable. In particular, p-Met resulted expressed in exosomes of castration-resistant patients. miR-130b is highly expressed in exosomes isolated from castration-resistant patients (data not shown). This suggests that it is possible to monitor metastatic patients and a dedicated study will be performed to correlate p-Met/miR-130b level and therapeutic benefit of Met inhibitor treatment in this setting of patients. Our data suggest that miR-130b/p-Met axis contributes to increase recurrence risk and promotes tumor progression. Furthermore, we demonstrated that it is possible to monitor miR-130b and Met signaling cascade in vesicles isolated from peripheral blood both in pre-surgery candidates and castration-resistant patients. This may suggest new markers and methods for therapy decision-making in all phases of the disease and may add molecular information for designing dedicated clinical trials.

MiR-130b and c-Met expression evaluated in an *ex vivo* cellular model of human PCa

As validation on an independent cohort of PCa patients with long (10 years) and well-defined follow-up, we took benefit of the established *ex vivo* models, published by Nanni *et al.*[39] We evaluated miR-130b level in cancer primary cultures isolated from patients with well-documented prognosis. In detail, we revealed the expression of miR-130b in 18 cultures (4 normal/hyperplasia-derived cells; 7 tumor-derived cells with good prognosis; 7 tumor-derived cells with poor prognosis). We found a significant increase of miR-130b in the poor prognosis group (Supplementary Figure 5a). Moreover, c-MET gene expression, evaluated reanalyzing data published in Nanni S *et al.*, by the Affymetrix Human U133A Gene Chip platform, significantly correlated with high levels of miR-130b (Supplementary Figure 5b). The significant increase of miR-130b and c-Met in cells from patients with poor prognosis was confirmed in this model by single RT-PCR and cytofluorimetric analysis, respectively (Supplementary Figure 5c). To disclose the functional role of miR-130b, we transfected the poor prognosis cell line C11IM with anti-miRNA-130b oligo. After miR-130b repression, C11IM showed a modest AR de-repression and a consistent reduction of anti-apoptotic genes (Supplementary Figures 6a and b). However, cancer cells did not affect their proliferation rate (data not shown), suggesting that miR-130b inhibition is insufficient to exert a therapeutic effect. Then, we treated C11IM with the specific c-Met inhibitor SU11274, which promoted miR-130b reduction and consistent cell growth decrease (Supplementary Figures 6c and d). These data suggest that c-Met/miR-130b axis synergistically may concur to therapy resistance and cancer progression.

MiR-130b *in vitro* and *in vivo* analysis in PCa

To investigate whether miR-130b was the mediator of c-Met aberrant activity, we overexpressed the miRNA in LNCaP cells, which retain miR-130b expression at the same low level as

non-neoplastic cells (Supplementary Figure 2b). We amplified miR-130b gene from normal human genome and sub-cloned it into the TWEEN (TW) lentiviral vector for stable delivery.[23] LNCaP cells were transduced with miRNA (LNCaP/TW-miR-130b) and relative empty vector control (LNCaP/TW), both carrying the enhanced green fluorescence protein (EGFP) reporter (Figure 3a). MiR-130b overexpression was confirmed by qRT-PCR assay (Supplementary Figure 7a). AR protein amount was reduced in parallel with miR-130b overexpression (Supplementary Figure 7b). MiR-130b increased level did not significantly influence

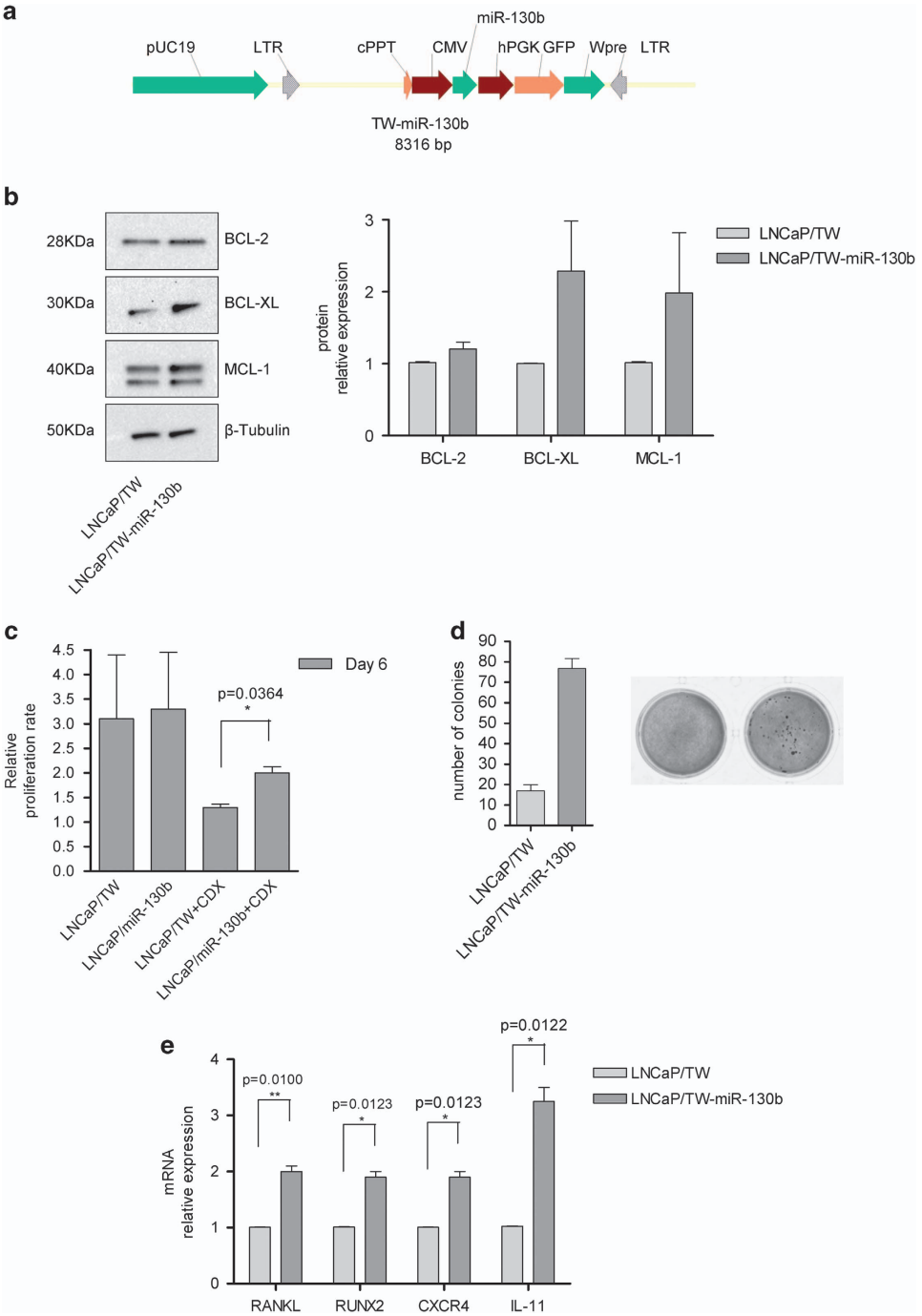

Figure 3. (**a**) Schematic representation of TWEEN lentiviral vector carrying the genomic region encoding for miR-130b. (**b**) Representative Western blot showing BCL-2, Bcl-XL and Mcl-1 expression levels in miR-130b-overexpressing LNCaP cells (TW-miR-130b) and relative controls (TW). β—Tubulin was used as a loading control. Histograms show mean ± s.d. of three independent experiments. (**c**) Proliferation analysis ($P = 0.03$) of LNCaP/miR-130b versus control cells treated with 5 μM of Casodex (CDX) after 6 days of treatment expressed as fold change over day 0 plating cell concentration. Data are shown as mean ± s.d. of three independent experiments. (**d**) Representative image showing differences in colony formation properties between miR-130b-overexpressing (TW-miR-130b) LNCaP cells and relative controls TWEEN (TW). Histogram data (**e**) real-time PCR analysis of RANKL ($P = 0.01$), RUNX-2 ($P = 0.0123$), CXCR-4 ($P = 0.0123$) and IL-11 ($P = 0.0122$) relative expression in LNCaP/miR-130b and control cells LNCaP/TW. Data are shown as mean ± s.d. of three independent experiments performed in three replicates.

proliferation rate *per se* (data not shown). Thus, we speculated a possible role of the miRNA in survival and invasion tumor capability. Western blot analysis showed that the expression of anti-apoptotic genes BCL-2, BcL-XL and Mcl-1 was considerably upregulated (Figure 3b). We speculated that the increased level of anti-apoptotic genes mediated by miR-130b was associated with resistance to therapy. In particular, we thought that miR-130b/Met axis aberrant expression may be involved in the acquisition of castration resistance state. To evaluate this hypothesis, we mirrored patient hormone deprivation treatment conventionally used after evidence of tumor recurrence. We treated miR-130b-overexpressing LNCaP cells (LNCaP/TW-miR-130b) and their relative controls (LNCaP/TW) with 5 μM of non-steroideal antiandrogen Casodex (CDX). We revealed a significant resistance of miR-130b-overexpressing cells to drug cell death induction (LNCaP/TW-miR-130b) compared with LNCaP/TW controls (Figure 3c). These results suggest that deregulation of miR-130b/Met axis may be a novel mechanism for a more aggressive tumor phenotype acquisition during HT treatment. We performed soft-agar culture of miR-130b-overexpressing LNCaP cells (LNCaP/TW-miR-130b) and their relative controls (LNCaP/TW). The assay revealed consistent anchorage-independent and clonogenic capacities of LNCaP/miR-130b cells, compared with their relative controls (Figure 3d). Furthermore, miR-130b-overexpressing LNCaP cells showed the ability of matrix digestion and spreading into agar underlying invasive property acquisition (Supplementary Figure 7c). Of note, LNCaP/TW-miR-130b cells were characterized by the overexpression of genes correlated with metastatic spreading at messenger RNA level (Figure 3e), such as IL-11, CXCR-4, RUNX-2 and RANKL,[47–50] indicating that miR-130b could be a putative promoter of bone metastasis formation. We overexpressed miR-130b in two additional tumor models, 22Rv1 cells and the *ex vivo* primary cell line C41IM, obtained from good prognosis patient tissue (Supplementary Figures 1a and b; Supplementary Figure 5). 22Rv1 and C41IM cells showed AR reduction after miR-130b overexpression (Supplementary Figures 8a–c), together with increase in migratory capacity and invasion gene activation (Supplementary Figures 8d–f). To determine whether miR-130b forced expression could affect tumor development *in vivo*, we orthotopically injected miR-130b-overexpressing LNCaP cells (LNCaP/TW-miR-130b) and their relative controls (LNCaP/TW) in NSG (NOD.Cg-*Prkdc*^{scid} *Il2rg*^{tm1Wjl}/SzJ) mice. Four weeks post injection, 90% of LNCaP/TW-miR-130b inoculated mice showed tumor engraftment, whereas only 25% of LNCaP/TW control mice had signals as by *in vivo* imaging system (IVIS) analysis (Figure 4a). At eight weeks, luciferase activity was considerably higher in mice carrying LNCaP/miR-130b as compared with LNCaP/TW xenografts (data not shown), indicating that miR-130b overexpression accelerated tumor propagation. Accordingly, LNCaP/miR-130b explanted tumors showed a pronounced front of invasion, while LNCaP/TW tumors seemed more confined (Figure 4a). To investigate the *in vivo* effect of miR-130b upregulation on tumor cell survival, homing and spreading, we inoculated LNCaP/TW and LNCaP/miR-130b cells into the left ventricle of NSG mice. After 10 weeks from injection, 70% of mice treated with LNCaP/miR-130b cells showed homing capacity in distant districts (Figure 4b). The lesion masses were consistently visible under stereomicroscope such as EGFP images paralleling with imaging signals (Figure 4b right panel and Supplementary Figure 9a). On the contrary, LNCaP/TW cells were able to give signals without large masses visible at stereomicroscopic analysis only in 25% of inoculated mice. Thus, these experiments demonstrated the capability of miR-130b-overexpressing cells to survive in blood flow, invade organs and form lesions. As miR-130b high levels promoted cancer progression and miR-130b is increasingly upregulated in tumor and in metastatic samples from PCa patients (Figure 2a), we next investigated the possible prognostic value of miR-130b levels. The analysis on Taylor's data set showed that patients with higher level of miR-130b had significant probability of tumor recurrence and a reduced disease-free time (Figures 4c and d). To validate these data, we ran a (additional to Figure 2d) pivotal analysis on nine microdissected (only tumor cells were laser dissected) formalin-fixed, paraffin-embedded primary tumors with documented 10-year follow-up and we evaluated miR-130b level by RT-PCR. Five of the seven patients who developed metastases had high levels of miR-130b, whereas the two free of recurrence had low miR levels (Supplementary Figure 9b). Based on these results, we hypothesized a sophisticate mechanism where c-Met is able to regulate AR through miR-130b induction and this aberrant circuitry leads to a more aggressive phenotype. Our data propose Met/miR-130 axis as possible marker for monitoring cancer progression and for optimizing therapy decision.

DISCUSSION

PCa has an incidence of ~37% in men in western countries. Many tumors remain indolent, whereas others acquire aggressive phenotype. Studies conducted on people dying from different causes showed that ~60–70% of older men have histological indolent PCa.[1,20,51–53] For reducing the risk of overtreatment in patients with indolent forms, two conservative management strategies of 'watchful waiting' and 'active surveillance' have been proposed. However, there are not enough reliable biomarkers to distinguish the tumors that will remain indolent from those that will progress. The ability to ameliorate risk assessment and individuate indolent forms may amplify the opportunity to drive patients to active surveillance or to the right treatment.[52,53] On the other hand, a consistent fraction of patients with organ-confined tumors will develop advanced forms. The number of new diagnosed cancers per year is increasing, mainly as a result of prostate-specific antigen screening and 'multicore' schemes of prostate biopsy, whereas the probability to develop advanced form is not decreasing. Thus, this suggests that many men with localized PCa would not entirely benefit from radical treatment. An elevated percentage of patients at high risk and a consistent fraction of low/medium-risk patients show evidence of tumor recurrence in few years. After hormone ablation therapy, the majority of advanced forms acquires resistance to castration and evolve to unresponsive tumors. The discovery of new mechanisms of cancer progression and HT escaping may suggest novel biomarkers for monitoring of patients and new therapeutic approaches. In this study, we investigate the cooperation between AR and c-Met genes in developing therapy-resistant tumors. In particular, we demonstrated that c-Met is able to regulate AR expression through the induction of miR-130b. Although the role of miR-130b in cancer is debated, our hypothesis is that its function may be influenced by type and molecular context of the studied cancer.[36–38,54–57] It is likely that the HT causes AR activity reduction with consequent activation of c-Met transcription and expression. Such aberrant c-Met activity then upregulates miR--130b, which in turn inhibits AR at translation level. Furthermore, our data showed miR-130b *per se* stimulates apoptosis resistance and invasion capability of the tumor cells.

It is reported that AR can negatively control c-Met at transcriptional level.[21,22] Our results elucidated a novel circuitry where c-Met can regulate AR. Here we demonstrated a sophisticated regulation mechanism involving the direct control of c-Met on miR-130b expression level and the targeting of miR-130b on AR 3'UTR. High miR-130b levels significantly correlate with tumor and metastasis development, whereas miR-130b expression increases in parallel with conventional risk assessment parameters, Gleason and Stage. We demonstrated that miR-130b upregulation promotes invasion and resistance to therapy in LNCaP cells, suggesting that miR-130b has a key role in cancer progression. We showed that it is possible to analyze p-Met and

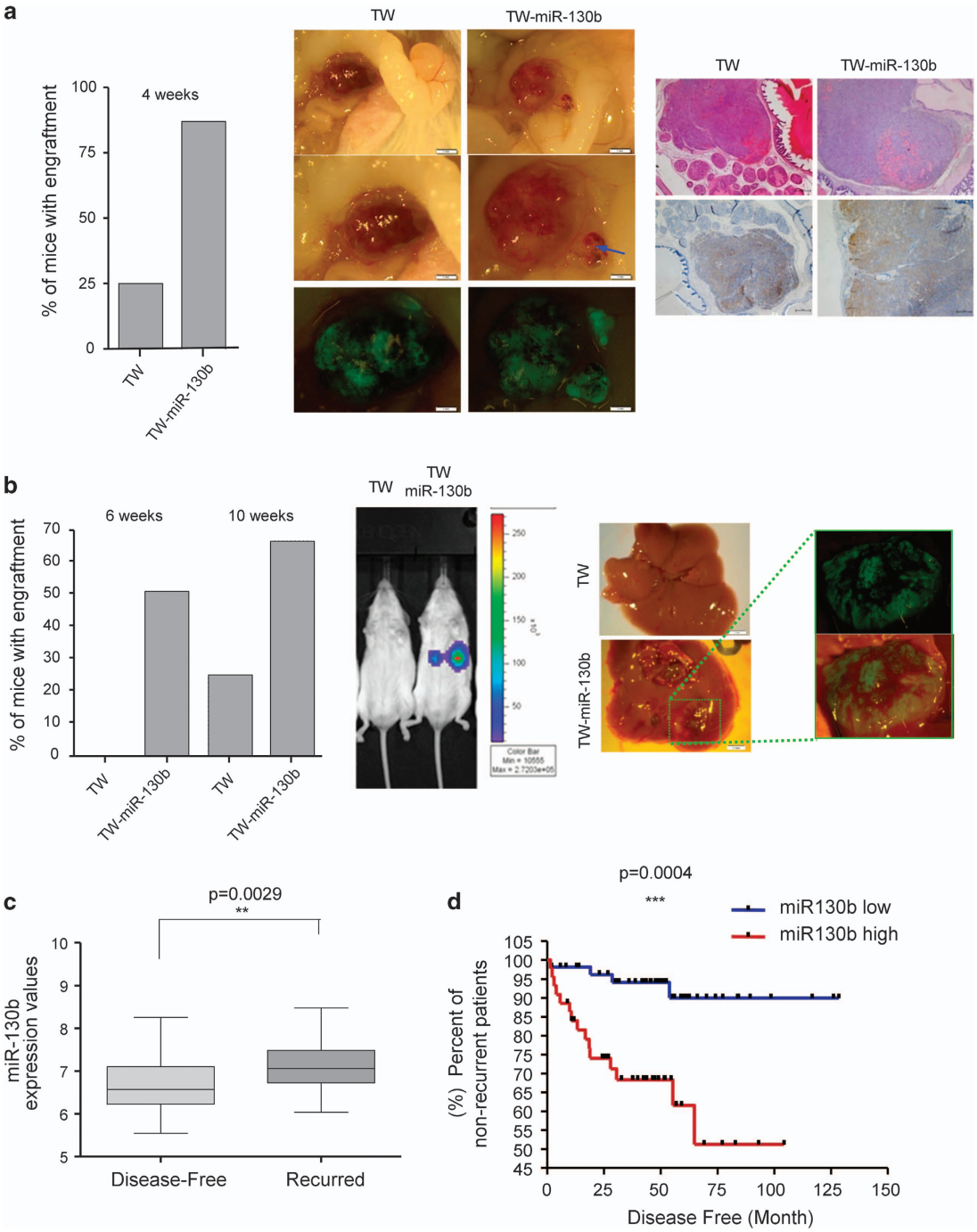

Figure 4. (**a**) Orthotopic injection of LNCaP/miR-130b (TW-miR-130b) and control cells (TW). Histograms represent the percentage of mice showing luciferase activity 4 weeks after orthotopic injection. In the left panel, images of tumors grown into murine prostate by stereomicroscopy analysis were reported. EGFP evaluation reveled human cells. Blue arrow indicates extra-primary mass invasive tumor area. Scale bars represent 1 mm. In the right panel, hematoxylin and eosin (H&E) and anti-human PSA stainings of TW and TW-miR-130b LNCaP tumors grown into murine prostate are shown. Scale bars represent 30 μm. Sixteen mice in two independent experiments were used. (**b**) Intracardiac injection of LNCaP/miR-130b (TW-miR-130b) and control cells (TW). Percentage of mice showing luciferase activity 6 and 9 weeks after injection. Luciferase activity was evaluated by *in vivo* imaging system imaging system. Representative image of luciferase activity in mice injected intracardiacally with transduced cells (TW or TW-miR-130b) as by *in vivo* imaging system imaging system. Representative image of explanted liver showing EGFP metastatic foci in miR-130b-overexpressing cells as by stereomicroscope analysis. Fourteen mice in two independent experiments were used. (**c**) *In silico* analysis of miR-130b expression levels in disease-free ($n = 80$) versus recurred patients ($n = 19$) in Taylor's data set. Mann–Whitney *U*-test was used to determine significance. (**d**) Kaplan–Meier survival curves of prostate cancer patients elaborated from Taylor's data set (clinical variable = disease-free survival) as a function of miR-130b-high ($n = 44$) versus miR-130b-low ($n = 55$) expressing tumors. Log-rank test was used to determine significance.

miR-130b levels in released exosomes isolated from peripheral blood of patients with primary and advanced PCas, suggesting that it is theoretically possible to perform patient monitoring by peripheral blood analysis. Our data suggest that this approach might be exploited for monitoring patients who will develop recurrence and therapy-resistant forms. As the tumor molecular setting can evolve, and metastases are molecularly different from the primary tumor, this approach may offer a source of material for dynamic monitoring and therapy adaptation.

We showed that c-Met inhibitors downregulate miR-130b in cell lines expressing high levels of the miR, thus suggesting an alternative strategy to target miR-130b in PCa. Administration of targeted or conventional therapies requires accuracy of staging procedures and biomarkers predictive of patients' response. The functional roles of miRNAs in tumor biology is deeply investigated, and many evidences report that tissue or blood-based miRNA biomarkers that predict clinical behavior and/or therapeutic response can be used as prognostic and predictive biomarkers. Thus, our data suggest that it might be possible to monitor patients during therapy with non-invasive tests through the analysis of exosomes. If validated in adequately powered clinical trials, our results may provide a rationale for active surveillance clinical trials and allow to optimize advanced patient selection in clinical studies for therapy with new agents.

CONCLUSIONS

PCa is the most frequent tumor in men, the majority of cases being indolent. However, the mechanisms responsible for PCa progression remain to be elucidated. Our data propose new potential molecular markers able to identify patients at low and high risk of progression and who will escape from HT response. Furthermore, our results suggest that the analysis of the miR-130b/Met axis may provide indication to select candidate patients for Met inhibitor therapy.

MATERIALS AND METHODS

Cell culture and treatments

RWPE-1, RWPE-2, 22Rv1, LNCaP, PC-3 and DU145 were provided from American Type Culture Collection and cultivated in the recommended medium.

Data set elaboration

MicroRNA, messenger RNA and clinical data from Taylor's data set (NCBI GEO accession code GSE21032) have been accessed and explored through the MSKCC PCa Genomics Data Portal (http://cbio.mskcc.org/prostate-portal/). For additional details, see Supplementary Materials and Methods

CONFLICT OF INTEREST

The authors declare no conflict of interest.

ACKNOWLEDGEMENTS

We thank Giuseppe Loreto and Tania Merlino for their technical support. We thank Alessandra Boe for cytofluorimetric analysis. This manuscript was supported by National Ministry of Health, Under-forty researcher (2012) and Italy-USA microRNA program to DB and the Italian Association for Cancer (AIRC) and Fondazione Roma funding to RDM.

REFERENCES

1 Haas GP, Delongchamps N, Brawley OW, Wang CY, de la Roza G. The worldwide epidemiology of prostate cancer: perspectives from autopsy studies. *Can J Urol* 2008; **15**: 3866–3871.
2 Jemal A, Siegel R, Ward E, Murray T, Xu J, Smigal C *et al.* Cancer statistics, 2006. *CA Cancer J Clin* 2006; **56**: 106–130.
3 Isaacs JT, Coffey DS. Adaptation versus selection as the mechanism responsible for the relapse of prostatic cancer to androgen ablation therapy as studied in the Dunning R-3327-H adenocarcinoma. *Cancer Res* 1981; **41**(12 Pt 1): 5070–5075.
4 de Bono JS, Logothetis CJ, Molina A, Fizazi K, North S, Chu L *et al.* Abiraterone and increased survival in metastatic prostate cancer. *N Engl J Med* 2011; **364**: 1995–2005.
5 Scher HI, Fizazi K, Saad F, Taplin ME, Sternberg CN, Miller K *et al.* Increased survival with enzalutamide in prostate cancer after chemotherapy. *N Engl J Med* 2012; **367**: 1187–1197.
6 Balk SP. Androgen receptor as a target in androgen-independent prostate cancer. *Urology* 2002; **60**(3 Suppl 1): 132–138; discussion 138–139.
7 Feldman BJ, Feldman D. The development of androgen-independent prostate cancer. *Nat Rev Cancer* 2001; **1**: 34–45.
8 Gelmann EP. Molecular biology of the androgen receptor. *J Clin Oncol* 2002; **20**: 3001–3015.
9 Matias PM, Carrondo MA, Coelho R, Thomaz M, Zhao XY, Wegg A *et al.* Structural basis for the glucocorticoid response in a mutant human androgen receptor (AR (ccr)) derived from an androgen-independent prostate cancer. *J Med Chem* 2002; **45**: 1439–1446.
10 Taplin ME, Bubley GJ, Ko YJ, Small EJ, Upton M, Rajeshkumar B *et al.* Selection for androgen receptor mutations in prostate cancers treated with androgen antagonist. *Cancer Res* 1999; **59**: 2511–2515.
11 Taplin ME, Bubley GJ, Shuster TD, Frantz ME, Spooner AE, Ogata GK *et al.* Mutation of the androgen-receptor gene in metastatic androgen-independent prostate cancer. *N Engl J Med* 1995; **332**: 1393–1398.
12 Taplin ME, Rajeshkumar B, Halabi S, Werner CP, Woda BA, Picus J *et al.* Androgen receptor mutations in androgen-independent prostate cancer: Cancer and Leukemia Group B Study 9663. *J Clin Oncol* 2003; **21**: 2673–2678.
13 Veldscholte J, Ris-Stalpers C, Kuiper GG, Jenster G, Berrevoets C, Claassen E *et al.* A mutation in the ligand binding domain of the androgen receptor of human LNCaP cells affects steroid binding characteristics and response to anti-androgens. *Biochem Biophys Res Commun* 1990; **173**: 534–540.
14 Visakorpi T, Hyytinen E, Koivisto P, Tanner M, Keinanen R, Palmberg C *et al.* In vivo amplification of the androgen receptor gene and progression of human prostate cancer. *Nat Genet* 1995; **9**: 401–406.
15 Craft N, Shostak Y, Carey M, Sawyers CL. A mechanism for hormone-independent prostate cancer through modulation of androgen receptor signaling by the HER-2/neu tyrosine kinase. *Nat Med* 1999; **5**: 280–285.
16 Gioeli D, Ficarro SB, Kwiek JJ, Aaronson D, Hancock M, Catling AD *et al.* Androgen receptor phosphorylation. Regulation and identification of the phosphorylation sites. *J Biol Chem* 2002; **277**: 29304–29314.
17 Gregory CW, Johnson Jr RT, Mohler JL, French FS, Wilson EM. Androgen receptor stabilization in recurrent prostate cancer is associated with hypersensitivity to low androgen. *Cancer Res* 2001; **61**: 2892–2898.
18 Li P, Yu X, Ge K, Melamed J, Roeder RG, Wang Z. Heterogeneous expression and functions of androgen receptor co-factors in primary prostate cancer. *Am J Pathol* 2002; **161**: 1467–1474.
19 Brawn PN, Speights VO. The dedifferentiation of metastatic prostate carcinoma. *Br J Cancer* 1989; **59**: 85–88.
20 Jemal A, Bray F, Center MM, Ferlay J, Ward E, Forman D. Global cancer statistics. *CA Cancer J Clin Mar-Apr* **61**: 69–90.
21 Maeda A, Nakashiro K, Hara S, Sasaki T, Miwa Y, Tanji N *et al.* Inactivation of AR activates HGF/c-Met system in human prostatic carcinoma cells. *Biochem Biophys Res Commun* 2006; **347**: 1158–1165.
22 Verras M, Lee J, Xue H, Li TH, Wang Y, Sun Z. The androgen receptor negatively regulates the expression of c-Met: implications for a novel mechanism of prostate cancer progression. *Cancer Res* 2007; **67**: 967–975.
23 Bonci D, Coppola V, Musumeci M, Addario A, Giuffrida R, Memeo L *et al.* The miR-15a-miR-16-1 cluster controls prostate cancer by targeting multiple oncogenic activities. *Nat Med* 2008; **14**: 1271–1277.
24 Calin GA, Croce CM. MicroRNA signatures in human cancers. *Nat Rev Cancer* 2006; **6**: 857–866.
25 Esquela-Kerscher A, Slack FJ. Oncomirs - microRNAs with a role in cancer. *Nat Rev Cancer* 2006; **6**: 259–269.
26 Garofalo M, Romano G, Di Leva G, Nuovo G, Jeon YJ, Ngankeu A *et al.* EGFR and MET receptor tyrosine kinase-altered microRNA expression induces tumorigenesis and gefitinib resistance in lung cancers. *Nat Med Jan* **18**: 74–82.
27 Niu Y, Altuwaijri S, Lai KP, Wu CT, Ricke WA, Messing EM *et al.* Androgen receptor is a tumor suppressor and proliferator in prostate cancer. *Proc Natl Acad Sci USA* 2008; **105**: 12182–12187.
28 Tilley WD, Wilson CM, Marcelli M, McPhaul MJ. Androgen receptor gene expression in human prostate carcinoma cell lines. *Cancer Res* 1990; **50**: 5382–5386.

29 Knudsen BS, Edlund M. Prostate cancer and the met hepatocyte growth factor receptor. *Adv Cancer Res* 2004; **91**: 31–67.
30 Nguyen HM, Ruppender N, Zhang X, Brown LG, Gross TS, Morrissey C *et al.* Cabozantinib inhibits growth of androgen-sensitive and castration-resistant prostate cancer and affects bone remodeling. *PloS One* 2013; **8**: e78881.
31 Varkaris A, Corn PG, Gaur S, Dayyani F, Logothetis CJ, Gallick GE. The role of HGF/c-Met signaling in prostate cancer progression and c-Met inhibitors in clinical trials. *Expert Opin Investig Drugs* 2011; **20**: 1677–1684.
32 Verhoef EI, Kolijn K, De Herdt MJ, van der Steen B, Hoogland AM, Sleddens HF *et al.* MET expression during prostate cancer progression. *Oncotarget* 2016; **7**: 31029–31036.
33 Taylor BS, Schultz N, Hieronymus H, Gopalan A, Xiao Y, Carver BS *et al.* Integrative genomic profiling of human prostate cancer. *Cancer Cell* 2010; **18**: 11–22.
34 Dean M, Park M, Kaul K, Blair D, Vande Woude GF. Activation of the met proto-oncogene in a human cell line. *Haematol Blood Transfus* 1987; **31**: 464–468.
35 Dean M, Park M, Vande Woude GF. Characterization of the rearranged tpr-met oncogene breakpoint. *Mol Cell Biol* 1987; **7**: 921–924.
36 Li BL, Lu C, Lu W, Yang TT, Qu J, Hong X *et al.* miR-130b is an EMT-related microRNA that targets DICER1 for aggression in endometrial cancer. *Med Oncol* 2013; **30**: 484.
37 Liu AM, Yao TJ, Wang W, Wong KF, Lee NP, Fan ST *et al.* Circulating miR-15b and miR-130b in serum as potential markers for detecting hepatocellular carcinoma: a retrospective cohort study. *BMJ Open* 2012; **2**: e000825.
38 Ma S, Tang KH, Chan YP, Lee TK, Kwan PS, Castilho A *et al.* miR-130b Promotes CD133(+) liver tumor-initiating cell growth and self-renewal via tumor protein 53-induced nuclear protein 1. *Cell Stem Cell* 2010; **7**: 694–707.
39 Nanni S, Priolo C, Grasselli A, D'Eletto M, Merola R, Moretti F *et al.* Epithelial-restricted gene profile of primary cultures from human prostate tumors: a molecular approach to predict clinical behavior of prostate cancer. *Mol Cancer Res* 2006; **4**: 79–92.
40 Reisinger K, Kaufmann R, Gille J. Increased Sp1 phosphorylation as a mechanism of hepatocyte growth factor (HGF/SF)-induced vascular endothelial growth factor (VEGF/VPF) transcription. *J Cell Sci* 2003; **116**(Pt 2): 225–238.
41 Mueller C, Edmiston KH, Carpenter C, Gaffney E, Ryan C, Ward R *et al.* One-step preservation of phosphoproteins and tissue morphology at room temperature for diagnostic and research specimens. *PloS One* 2011; **6**: e23780.
42 Pierobon M, Wulfkuhle J, Liotta L, Petricoin E. Application of molecular technologies for phosphoproteomic analysis of clinical samples. *Oncogene* 2015; **34**: 805–814.
43 Boeri M, Verri C, Conte D, Roz L, Modena P, Facchinetti F *et al.* MicroRNA signatures in tissues and plasma predict development and prognosis of computed tomography detected lung cancer. *Proc Natl Acad Sci USA* 2011; **108**: 3713–3718.
44 Melo SA, Sugimoto H, O'Connell JT, Kato N, Villanueva A, Vidal A *et al.* Cancer exosomes perform cell-independent microRNA biogenesis and promote tumorigenesis. *Cancer Cell* 2014; **26**: 707–721.
45 Sozzi G, Boeri M, Rossi M, Verri C, Suatoni P, Bravi F *et al.* Clinical utility of a plasma-based miRNA signature classifier within computed tomography lung cancer screening: a correlative MILD trial study. *J Clin Oncol* 2014; **32**: 768–773.
46 Federici G, Gao X, Slawek J, Arodz T, Shitaye A, Wulfkuhle JD *et al.* Systems analysis of the NCI-60 cancer cell lines by alignment of protein pathway activation modules with '-OMIC' data fields and therapeutic response signatures. *Mol Cancer Res* 2013; **11**: 676–685.
47 Blyth K, Cameron ER, Neil JC. The RUNX genes: gain or loss of function in cancer. *Nat Rev Cancer* 2005; **5**: 376–387.
48 Jones DH, Nakashima T, Sanchez OH, Kozieradzki I, Komarova SV, Sarosi I *et al.* Regulation of cancer cell migration and bone metastasis by RANKL. *Nature* 2006; **440**: 692–696.
49 Kang Y, Siegel PM, Shu W, Drobnjak M, Kakonen SM, Cordon-Cardo C *et al.* A multigenic program mediating breast cancer metastasis to bone. *Cancer Cell* 2003; **3**: 537–549.
50 Wang J, Loberg R, Taichman RS. The pivotal role of CXCL12 (SDF-1)/CXCR4 axis in bone metastasis. *Cancer Metastasis Rev* 2006; **25**: 573–587.
51 Adolfsson J. Watchful waiting and active surveillance: the current position. *BJU Int* 2008; **102**: 10–14.
52 D'Amico AV, Chen MH, Roehl KA, Catalona WJ, Preoperative PSA. velocity and the risk of death from prostate cancer after radical prostatectomy. *N Engl J Med* 2004; **351**: 125–135.
53 D'Amico AV, Moul J, Carroll PR, Sun L, Lubeck D, Chen MH. Prostate specific antigen doubling time as a surrogate end point for prostate cancer specific mortality following radical prostatectomy or radiation therapy. *J Urol* 2004; **172**(5 Pt 2): S42–S46; discussion S6–7.
54 Colangelo T, Fucci A, Votino C, Sabatino L, Pancione M, Laudanna C *et al.* MicroRNA-130b promotes tumor development and is associated with poor prognosis in colorectal cancer. *Neoplasia* 2013; **15**: 1218–1231.
55 Dong P, Karaayvaz M, Jia N, Kaneuchi M, Hamada J, Watari H *et al.* Mutant p53 gain-of-function induces epithelial-mesenchymal transition through modulation of the miR-130b-ZEB1 axis. *Oncogene* 2013; **32**: 3286–3295.
56 Su X, Chakravarti D, Cho MS, Liu L, Gi YJ, Lin YL *et al.* TAp63 suppresses metastasis through coordinate regulation of Dicer and miRNAs. *Nature* 2010; **467**: 986–990.
57 Zhao G, Zhang JG, Shi Y, Qin Q, Liu Y, Wang B *et al.* MiR-130b is a prognostic marker and inhibits cell proliferation and invasion in pancreatic cancer through targeting STAT3. *PloS One* 2013; **8**: e73803.
58 Lewis BP, Burge CB, Bartel DP. Conserved seed pairing, often flanked by adenosines, indicates that thousands of human genes are microRNA targets. *Cell* 2005; **120**: 15–20.

Supplementary Information accompanies this paper on the Oncogene website (http://www.nature.com/onc)